High carbon dioxide uptake by subtropical forest ecosystems in the East Asian monsoon region

Q:1

Guirui Yu[a,1], Zhi Chen[a,b,1], Shilong Piao[c,d], Changhui Peng[e,f], Philippe Ciais[g], Qiufeng Wang[a], Xuanran Li[a], and Xianjin Zhu[a]

[a]Synthesis Research Center of Chinese Ecosystem Research Network, Key Laboratory of Ecosystem Network Observation and Modeling, Institute of Geographic Sciences and Natural Resources Research, Chinese Academy of Sciences, Beijing 100101, China; [b]University of Chinese Academy of Sciences, Beijing 100049, China; [c]Department of Ecology, College of Urban and Environmental Science, and Key Laboratory for Earth Surface Processes of the Ministry of Education, Peking University, Beijing 100871, China; [d]Laboratory of Alpine Ecology and Biodiversity, Institute of Tibetan Plateau Research, Chinese Academy of Sciences, Beijing 100101, China; [e]Department of Biology Sciences, Centre for Forest Research, University of Quebec at Montreal, Montreal, QC, Canada H3C 3P8; [f]State Key Laboratory of Soil Erosion and Dryland Farming on the Loess Plateau, College of Forestry, Northwest A and F University, Yangling, Shaanxi 712100, China; and [g]Laboratoire des Sciences du Climat et de l'Environnement, Commissariat à L'Energie Atomique, Centre National de la Recherche Scientifique, Université de Versailles Saint-Quentin-en-Yvelines (CEA-CNRS-UVSQ), 91191 Gif sur Yvette, France

Edited by Steven C. Wofsy, Harvard University, Cambridge, MA, and approved January 23, 2014 (received for review September 10, 2013)

Temperate- and high-latitude forests have been shown to contribute a carbon sink in the Northern Hemisphere, but fewer studies have addressed the carbon balance of the subtropical forests. In the present study, we integrated eddy covariance observations established in the 1990s and 2000s to show that East Asian monsoon subtropical forests between 20°N and 40°N represent an average net ecosystem productivity (NEP) of 362 ± 39 g C m^{-2} yr^{-1} (mean ± 1 SE). This average forest NEP value is higher than that of Asian tropical and temperate forests and is also higher than that of forests at the same latitudes in Europe–Africa and North America. East Asian monsoon subtropical forests have comparable NEP to that of subtropical forests of the southeastern United States and intensively managed Western European forests. The total NEP of East Asian monsoon subtropical forests was estimated to be 0.72 ± 0.08 Pg C yr^{-1}, which accounts for 8% of the global forest NEP. This result indicates that the role of subtropical forests in the current global carbon cycle cannot be ignored and that the regional distributions of the Northern Hemisphere's terrestrial carbon sinks are needed to be reevaluated. The young stand ages and high nitrogen deposition, coupled with sufficient and synchronous water and heat availability, may be the primary reasons for the high NEP of this region, and further studies are needed to quantify the contribution of each underlying factor.

Understanding the location of carbon sources and sinks and the underlying driving forces at scales ranging from local to global is crucial for accurately predicting future changes in atmospheric carbon dioxide and climate, and is helpful for defining management options for the global carbon cycle (1). In the Northern Hemisphere, mid- to high-latitude (40–60°N) terrestrial ecosystems have been shown to be carbon sink regions (2, 3), with a high carbon uptake by the large areas of temperate and boreal forests that are distributed from North America to Asiatic Russia (4). Tropical (0–20°N) forests in the Neotropics (5) and Africa (6) are also found to be carbon sinks. Conversely, the mid- to low-latitudes (20–40°N) of the American, European, and African continents include large areas under the control of the subtropical anticyclone that prevailing desert, steppe, and shrub ecosystems, such as the Sahara Desert, the Sonoran Desert, and the North American Prairie. Interestingly, the subtropical anticyclone zone also contains distinctive subtropical forests in the southeastern United States and East Asian monsoon region. There are large areas of subtropical forests in the East Asian monsoon region that benefit from the uplift of the Tibetan Plateau and the water supply furnished by the East Asian monsoon (*SI Appendix*, Fig. S1). The Tibetan Plateau (mean elevation over 4,000 m), acting as a strong heat source in summer, generates upward airflow motions over its eastern flank that, combined with large amounts of moisture from the tropics, result in strong monsoons and wet climate in East Asia (7, 8).

The approximate location of the East Asian monsoon region is latitude 20–40°N, longitude 100–145°E. This region includes the eastern part of China and the southern parts of Japan and Korea (9), and is characterized by wet, warm summer and dry, mild winter. The East Asian summer monsoon can bring large amounts of water vapor from the Pacific and Indian Oceans to the continent in summer, and the East Asian winter monsoon, driven by the Siberian high, brings large amounts of cold air to the continent in winter (Fig. 1). Forests in this region are typically composed of subtropical evergreen broad-leaved, deciduous broad-leaved, and mixed stands (10). Moderate resolution imaging spectroradiometer (MODIS) land-cover estimates indicate that the area of forest in the East Asian monsoon region increased from 2001 to 2010 (*SI Appendix*, Fig. S2). Furthermore, nitrogen deposition in this region has increased significantly, and it has been predicted to be one of the areas with the largest future increase in nitrogen deposition (11) (*SI Appendix*, Fig. S3). These changes are expected to cause a large carbon dioxide uptake by the forests in the East Asian monsoon region; however, there are limited data regarding the role of these forests in the global carbon cycle.

Here, we present estimates of the forest net ecosystem productivity (NEP) in the East Asian monsoon region based on a compilation of field observations using the eddy covariance technique during the period of the 1990s and 2000s. We analyzed 467 NEP records of 106 forest sites from ChinaFlux, AsiaFlux,

Significance

Understanding the location of carbon sources and sinks is essential for accurately predicting future changes in atmospheric carbon dioxide and climate. Mid- to high-latitude terrestrial ecosystems are well known to be the principal carbon sink regions, yet less attention has been paid to the mid- to low-latitude ecosystems. In this study, long-term eddy covariance observations demonstrate that there is a high carbon dioxide uptake (net ecosystem productivity) by the mid- to low-latitude East Asian monsoon subtropical forests that were shaped by the uplift of the Tibetan Plateau. Increasing nitrogen deposition, a young forest age structure, and sufficient water and heat availability combined to contribute to this large carbon dioxide uptake.

Author contributions: G.Y. designed research; Z.C., Q.W., X.L., and X.Z. collected data; Z.C. performed data analysis; and G.Y., Z.C., S.P., C.P., and P.C. wrote the paper.

The authors declare no conflict of interest.

This article is a PNAS Direct Submission.

[1]To whom correspondence may be addressed. E-mail: yugr@igsnrr.ac.cn or chenz.11b@igsnrr.ac.cn.

This article contains supporting information online at www.pnas.org/lookup/suppl/doi:10.1073/pnas.1317065111/-/DCSupplemental.

ECOLOGY

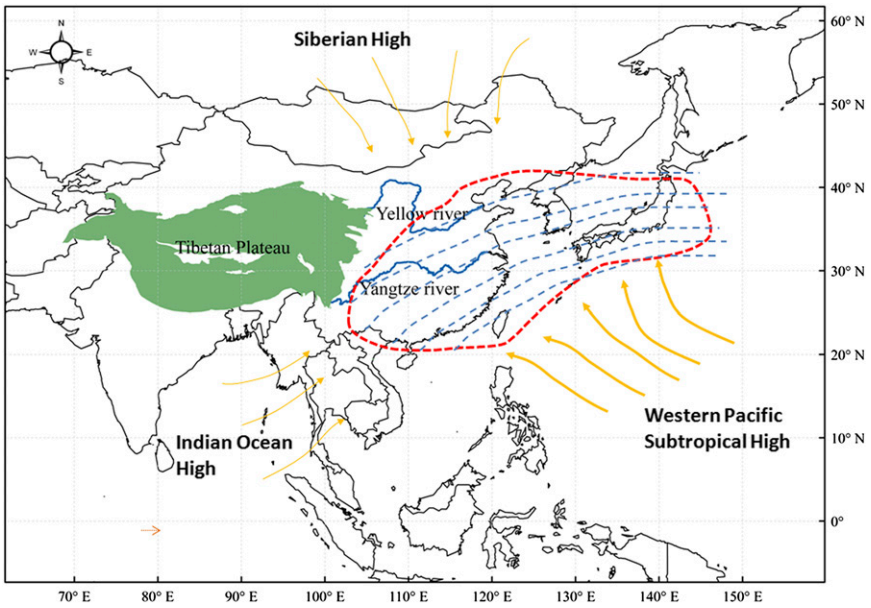

Fig. 1. Location of the East Asian monsoon region. The red circle and inner blue lines represent the East Asian monsoon region. The yellow arrows represent the Western Pacific subtropical high, Siberian high and Indian Ocean high. The green region indicates the Tibetan Plateau (9).

AmeriFlux, CarboEurope, and other networks, covering latitudes from 2° to 70°N and longitudes from 147°W to 143°E in the Northern Hemisphere (*SI Appendix*, Fig. S4 and Table S1). To better understand the importance of low-latitude Asian forests to the Northern Hemisphere land carbon uptake, we further investigated the determinants of NEP in the region and evaluated their impacts on NEP by comparing our eddy-covariance estimates with the results of three process-oriented models [Lund-Potsdam-Jena (LPJ) (12), Organizing Carbon and Hydrology In Dynamic Ecosystems (ORCHIDEE) (13), Community Land Model version 4-Carbon Nitrogen (CLM4CN) (14)] that have been used extensively in global terrestrial carbon flux evaluations (*Materials and Methods*).

Results and Discussion

By analyzing the latitudinal distribution of gross primary productivity (GPP), ecosystem respiration (RE), and NEP (Fig. 2), we found that the East Asian monsoon forests from 20°N to 40°N had the highest average NEP (Fig. 2*B*). The NEP values from 20°N to 30°N and from 30°N to 40°N reached 341 ± 67 ($n = 4$) and 368 ± 45 g C m^{-2} yr^{-1} ($n = 14$) (mean ± 1 SE), respectively, which are significantly higher than the corresponding values at low latitudes (0–20°N, 63 ± 52 g C m^{-2} yr^{-1}, $n = 5$, $P < 0.05$) and high latitudes (50–70°N, 127 ± 34 g C m^{-2} yr^{-1}, $n = 6$, $P < 0.05$) in Asia (Fig. 2 and *SI Appendix*, Table S2). Compared with average forest NEP at the same latitudes, the NEP of the East Asian monsoon forests is significantly higher than that of the Europe–Africa ($n = 2$, $P < 0.05$) (Fig. 3). The average NEP is close to the value measured in subtropical forests of the southeastern United States ($n = 3$, $P > 0.05$) (Fig. 3), but the latter forests exhibit a larger spatial variation in NEP from available eddy covariance data (Fig. 3). The magnitude of NEP in the East Asian monsoon region is comparable to the average NEP measured in intensively managed Western European forests between 40°N and 60°N (392 ± 47 g C m^{-2} yr^{-1}, $n = 19$) but much higher than the average NEP of Asian (157 ± 28 g C m^{-2} yr^{-1}, $n = 11$) and North American forests (180 ± 33 g C m^{-2} yr^{-1}, $n = 28$) between 40°N and 60°N (Fig. 3).

A deeper understanding of the driving forces underlying the high NEP values in the East Asian monsoon region is critical for understanding the mechanisms that control the terrestrial carbon cycle and the sustainability of the current carbon uptake. Previous studies indicated that recovery from past disturbance coupled to changes in disturbance regimes, plays an important role in controlling NEP variations (15–17). Because the age structure of

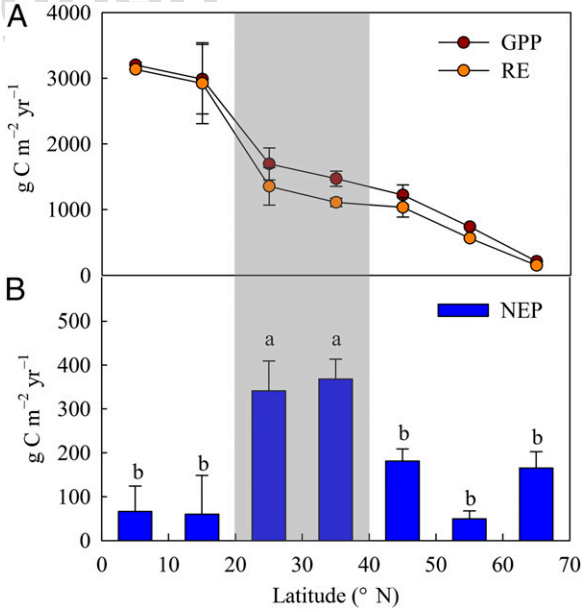

Fig. 2. Estimates of GPP, RE, and NEP for 10° latitude bins in the Asian region. (*A*) The seven bins indicate the latitudinal estimates of GPP and RE for Asian forest ecosystems from 0°N to 70°N. $n = 2, 3, 4, 7, 6, 1, 1$, respectively. (*B*) The seven bins indicate the latitudinal estimates of NEP for Asian forest ecosystems from 0°N to 70°N. $n = 2, 3, 4, 14, 9, 2, 4$, respectively. The circles or columns and bars represent the mean ± 1 SE. The different lowercase letters indicate values that differ significantly and are marked as a and b, successively. The average NEP of 20–40°N was significantly larger than that of other latitudes ($P < 0.05$), while the average NEP of 20–30°N was marginally larger than that in 40–50°N ($P = 0.056$) and in 60–70°N ($P = 0.073$). The average NEP in 50–60°N is not significantly different from that in 40–50°N or 60–70°N ($P > 0.1$).

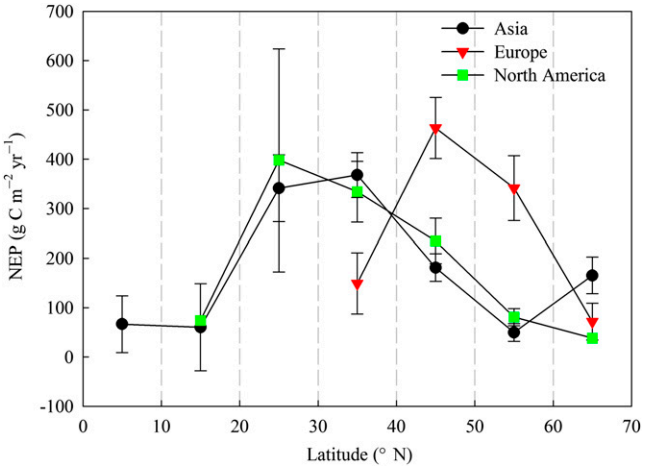

Fig. 3. Comparison of NEP for the Asian, European–African, and North American regions according to latitude. The points and bars represent the means ± 1 SE. The black points represent the Asian region, where n = 38, n = 2, 3, 4, 14, 9, 2, 4, respectively, for seven bins from 0°N to 70°N. The red triangles represent the European–African region, where n = 29, n = 2, 8, 11, 8, respectively, for four bins from 30°N to 70°N. The green squares represent the North American region, where n = 39, n = 1, 2, 7, 18, 10, 1, respectively, for six bins from 10°N to 70°N.

a forest is a simple and direct proxy for time since disturbance, we analyzed how forest age affects NEP. Integrating site-level, directly observed NEP, and forest age data, we found that NEP shows a clearly decreasing relationship with increasing forest age, although variation occurred within the age bands (Fig. 4*A*). Maximum NEP is observed in forests of less than 50 y, a phenomenon that is most likely a result of the high level of photosynthesis by young forests to produce biomass and structure that are consistently observed in tropical to boreal forests (18–20). In young forests, net primary productivity (NPP) exceeds heterotrophic respiration (R_h), resulting in high NEP, whereas in older stands, NPP may decline while R_h continues to increase because of the accumulation of detritus and soil organic matter from earlier production (21). Fig. 5*A* illustrates that the average stand age in the East Asian monsoon forests with eddy-covariance measurements, is significantly younger than those forests measured at other latitudes. At the regional scale, intensive afforestation and reforestation indeed have been conducted in the East Asian monsoon region since the 1960s. In particular, the area of plantation forest increased to 38.22 Mha and the area of secondary natural forest increased by 2.03 Mha in subtropical China from 2004 to 2008 (22). Planted and naturally regenerated forests are estimated to occupy 94%, 81%, and 52% of the area of forest in China, Japan, and Korea, respectively (23), and most of these planted and naturally regenerated forests are currently in the rapidly growing young- and middle-aged categories with high carbon uptake capacity (20, 24). High regional NEP is thus likely to prevail in the East Asian monsoon region given the absence of deforestation.

High nitrogen deposition may be another important factor driving the high NEP of the East Asian monsoon forest ecosystems. Direct information on the contribution of nitrogen deposition to NEP in the study region is, however, limited by the availability of colocated NEP and nitrogen deposition measurements. Here, we performed a spatial regression analysis between forest NEP and nitrogen deposition across Asian forest sites. The results show that forest NEP is positively correlated with nitrogen deposition (R^2 = 0.46; P = 0.0011) (Fig. 4*B* and *SI Appendix*, Table S3). Forest NEP thus covaries spatially with nitrogen deposition, although it should be noted that a statistically significant relationship does not necessarily imply causality. Importantly, the East Asian monsoon region has experienced a high rate of increase in nitrogen deposition because of rapid industrial and agricultural development and marked population expansion (11). In the 2000s, wet nitrogen deposition rates in the East Asian monsoon region averaged 22.64 ± 1.22 kg N ha^{-1} yr^{-1} (mean ± 1 SE) (*Materials and Methods*), significantly higher than that in tropical (0–20°N) and temperate (40–60°N) forests regions (Fig. 5*B*). Atmospheric deposition supplies large amounts of nitrogen to Asian subtropical forests, which are generally poor in soil organic carbon and nitrogen because of heavy leaching and fast mineralization (25). As a result, nitrogen inputs generally stimulate tree growth before nitrogen reaches saturation (26, 27), while altering soil respiration slightly or possibly limiting soil respiration on a long-term basis (28–30). An increasing nitrogen deposition trend is projected from emission scenarios prescribed to atmospheric chemistry models in Asia—particularly in East and South Asia—over the next 30 y (31, 32), which would act to continue increasing NEP (27).

Young age structure of forest stands and high nitrogen deposition have been identified as drivers of net carbon uptake by forests, but the magnitude of age and nitrogen deposition effect

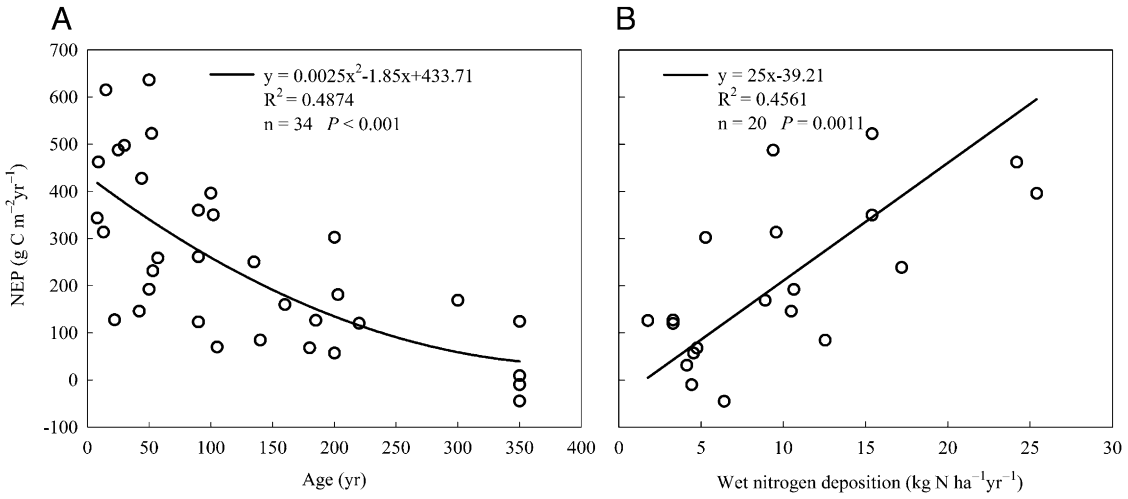

Fig. 4. Relationships between NEP and forest age and NEP and wet nitrogen deposition in the Asian region. (*A*) Correlation of NEP and forest age, n = 34, P < 0.001. (*B*) Correlation of NEP and wet nitrogen deposition, n = 20, P = 0.0011.

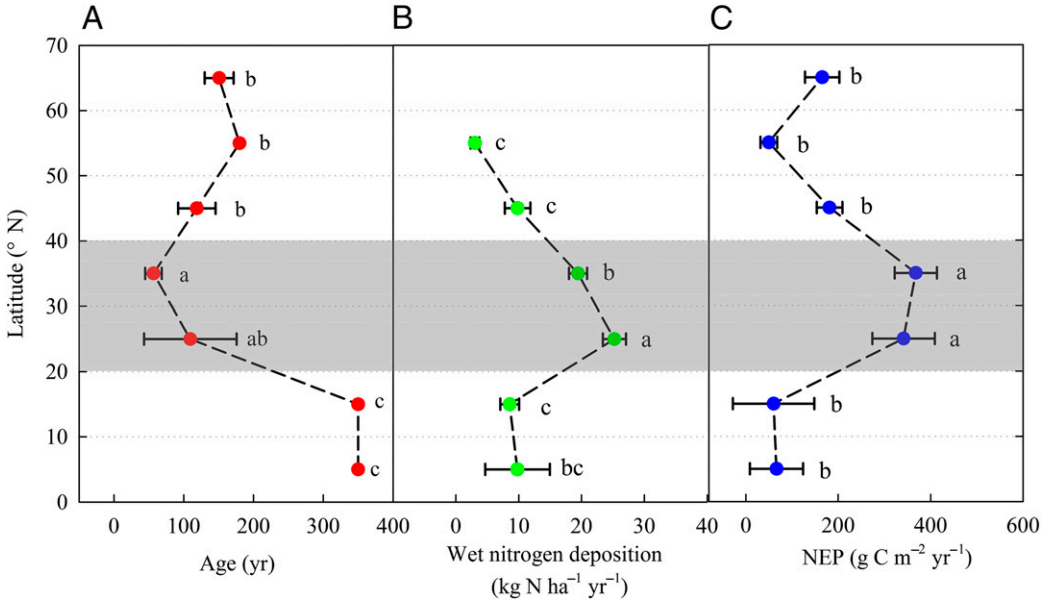

Fig. 5. Latitudinal distribution of NEP, wet nitrogen deposition and forest age in the Asian region. (*A*) The latitudinal distribution of forest age for Asian forest ecosystems between 0°N and 70°N. $n = 2, 2, 4, 12, 9, 2, 4$, respectively, for seven bins from 0°N to 70°N. (*B*) The latitudinal distribution of wet nitrogen deposition for Asian forest ecosystems between 0°N and 70°N. $n = 4, 13, 98, 80, 20, 5$, respectively, for six bins from 0°N to 60°N. (*C*) The latitudinal distribution of NEP for the Asian forest ecosystems between 0°N and 70°N. $n = 2, 2, 4, 14, 9, 2, 4$, respectively, for the seven bins from 0°N to 70°N. The circles and bars represent the mean ± 1 SE for 10° latitude bins. The values that differ significantly are labeled with different lowercase letters, marked as a, b, and c, successively ($P < 0.05$).

is associated with climate conditions. Young stands exhibit rapid growth, high carbon uptake corresponding to threshold values of high nitrogen addition; they also require sufficient light and water. The multivariate regression analysis indicates that age structure and nitrogen deposition coupled with favorable climate conditions explain more than 70% of the variation in NEP in Asia (*SI Appendix*, Table S4). The East Asian monsoon region between 20°N and 40°N is characterized by a subtropical humid monsoon climate, with humid summer and dry winter. Climate data indicate that the average temperature during the growing season (i.e., May–October) in forested areas of the East Asian monsoon region is ~20 °C, which is comparable with temperatures at the same latitudes of European–African (18 °C) and North American (21 °C) regions. However, average precipitation during the growing season in forested areas in the East Asian monsoon region is up to 1,020 mm, considerably higher than that at the same latitudes of European–African (260 mm) and North American (630 mm) regions (*SI Appendix*, Fig. S5). Such sufficient and synchronous water resources and temperature thus furnish a good foundation for forest growth and carbon uptake. Coupled with the rapidly growing young- and middle-aged structure and the increase in nitrogen deposition, these factors contribute to the high NEP of forests in the East Asian monsoon region.

By simply multiplying the averaged forest NEP of the East Asian monsoon region by the total forest area from MODIS land-cover data (197 Mha), the total NEP of the East Asian monsoon forests is estimated to be ~0.72 ± 0.08 Pg C yr^{-1} (mean ± 1 SE) [90% confidence interval (CI) 0.24–1.22] (*Materials and Methods*). This forest NEP represents 30% of the total Asian forest NEP (2.46 Pg C yr^{-1}) (CI 2.38–2.55) and 8% of the global forest NEP (8.95 Pg C yr^{-1}) (CI 8.79–9.13) (*Materials and Methods*). The regional NEP value is large relative to the forested area in this region (i.e., 5% of the global forest areas). Several uncertainties in our estimation of East Asian monsoon forest NEP may originate from random errors in eddy covariance measurements and from current limited sampling in forest demographics (different ages) and in time. In addition, there is a large uncertainty in our estimation of global and Asian forest NEP because of the relatively coarse spatial resolution of the climate fields and satellite fraction of absorbed photosynthetically active radiation (FAPAR) predictors (0.5°) and the biased sampling (33). Furthermore, it also should be noted that NEP is from eddy covariance techniques recording the net carbon dioxide exchange between the atmosphere and terrestrial ecosystem, which cannot be directly interpreted as an estimation of the forest carbon sink. To precisely assess the carbon sink of the Asian region, further consideration needs to be given to the precise regional distribution of forest age and other drivers, the effects of deforestation, and disturbance-induced mortality and subsequent carbon losses (34).

To better understand the contribution of forest age and nitrogen deposition to NEP, we further used three models [LPJ (12), ORCHIDEE (13) and CLM4CN (14)] to estimate the East Asian monsoon region NEP (35) and compared these estimates to the results of our study (*Materials and Methods*). These three models have been used extensively in the Fourth and Fifth Assessment Reports of the International Panel on Climate Change and in global terrestrial carbon budget evaluations (35–37). The results indicated that those three process-oriented models tend to underestimate the carbon uptake by five- to sevenfold (*SI Appendix*, Fig. S6). The most likely explanation of this substantial difference is that the models consistently assume that the ecosystem has approached an equilibrium state. This assumption obviously neglects age-structure–related effects. In addition, the significant role of nitrogen deposition in carbon uptake was not considered by most models. Incorporating forest age-driven growth and mortality, and the effects of nitrogen deposition on carbon storage in soils and biomass into calibrated process-based models, and further evaluating the contribution of each process, is greatly important for accurately evaluating the carbon balance of the East Asian monsoon subtropical forests.

Our quantitative evaluation indicated that East Asian monsoon forest ecosystems have one of the highest carbon uptakes of forests worldwide, and demonstrated that these monsoon forest ecosystems represent another large carbon uptake region in addition to those furnished by mid- and high-latitude European and North American forests. The large and expanding areas of

young planted and natural forests in subtropical Asia, combined with high and increasing nitrogen deposition, will cause these forests to continuously absorb substantial carbon in the future. These results underscore the need to reevaluate the geographic distribution of carbon sinks in Northern Hemisphere forest ecosystems by focusing on the carbon-cycle processes and regional carbon sinks in the low-latitude subtropical regions of Asia.

Materials and Methods

Flux Data Collection. We collected published annual carbon flux data measured by the eddy covariance technique during the period of the 1990s and 2000s for Asia, Europe, North America, and the parts of Africa and South America in the Northern Hemisphere. The average data-collection period for Asia, Europe, and North America was from roughly the same time period: 1999–2008, 1997–2006, and 1997–2006 (10–90th percentile), respectively.

Flux Data Observation. Continuous CO_2 and H_2O densities were measured using an infrared gas analyzer. Wind speed was measured using a 3D sonic anemometer at a sampling frequency of 10 or 20 Hz at flux sites. The data were filtered and corrected by individual researchers from each site, with coordinate rotation, Webb-Pearman-Leuning correction (38), storage flux calculation, outlier filtering, nighttime CO_2 flux correction (39), gap filling (40), and net ecosystem exchange flux partitioning into GPP and RE (39). Nighttime CO_2 eddy-covariance flux under low atmospheric turbulence conditions was filtered using site-specific thresholds of friction velocity (u^*) by individual site researchers. Detailed u^* information for the sites is provided in *SI Appendix*, Table S1.

Flux Data Selection. For the process of data selection, in addition to the requirement that the flux data must be subject to rigid correction and quality control, the data were required to satisfy the following criteria: (*i*) Flux data should be continuously available for more than 1 y. It was difficult to correctly measure the flux during wintertime at five sites [Huzhong (HZ), Yichun (YC), Daxinganling (DXAL), Zotino, and Tura]. At the Tura site, however, the winter CO_2 flux based on chamber measurements was shown to represent a negligible proportion of the annual flux (41). The Zotino site data for the nongrowing-season carbon fluxes were obtained by extrapolating the short-term nongrowing-season measurement (42). For the YC, HZ, and DXAL sites, we estimated that the nongrowing-season fluxes were ~40% of the growing-season fluxes based on the nearby Laoshan sites. Considering their negligible wintertime fluxes but high representativeness, the above five sites were accepted in our study. However, the annual value at these sites might overestimate the NEP because of the underestimation of RE during the dormant season. (*ii*) The site must have been undisturbed by fire, logging, or other serious disturbances for the past 10 y.

Flux Data Synthesis. Through the data-selection process outlined above, we ultimately selected 106 flux sites and 467 site-year records. The sites span latitudes from 2°N to 70°N and longitudes from 147°W to 143°E. The sites included 9 evergreen broad-leaved forests, 50 evergreen coniferous forests, 25 deciduous broad-leaved forests, 7 deciduous coniferous forests, and 15 mixed forests (International Geosphere-Biosphere Program). We then divided these data geographically to correspond to the Asian region, European region (including parts of North Africa), and North American region (including parts of South America) (*SI Appendix*, Fig. S4). For continuous observations, we calculated the multiple-year average value for each site. Finally, we averaged the data into 10° latitude bins for our integrated analysis.

Flux Data Sampling Time Analysis. To estimate the potential bias caused by incompletely uniform sampling time, we performed the same analysis using a subset of the data from the same period (2000–2005). As shown in *SI Appendix*, Fig. S7, a similar pattern was found by the eddy covariance data from the entire period of 1990–2010 and the common period of 2000–2005. This result suggests that the slightly different periods of collection in the three regions do not significantly affect our main conclusion.

Meteorological Data. Synchronous meteorological data were also measured and collected at the flux sites. For sites with missing meteorological data, we first used the observations from a neighboring meteorological station obtained from the global surface summary of daily data produced by the National Climatic Data Center (ftp://ftp.ncdc.noaa.gov/pub/data/gsod). For the remaining sites with missing data, we used the observation-based temperature and precipitation data available in the Climate Research Unit (CRU05) monthly climate dataset from the International Satellite Land Surface Climatology Project Π (http://daac.ornl.gov/cgi-bin/dsviewer.pl?ds_id=1015) to fill the gaps.

Forest Age Data. Information on the forest age structure for each study site was obtained from data collected through site investigations. However, if the forest age data were specified in terms of a range, we used the average value (e.g., 110 y old to represent a range of 100–120 y old). This format included the Kahokuk, Yamashiro, Gwangneung deciduous forest, Mongonmorit, and Spasskaya Pad Pine sites. If only a minimum forest age was given (e.g., more than 100 y old), we used the minimum value. This format included the Nagoya and Teshio sites. Additionally, certain sites, such as the primary tropical rain forests at the Pasoh, Lambir, Sakaerat, and Mae Klong sites, had no clearly specified age data. We assumed that these sites were older than 350 y because they were even older than the primary tropical rainforests at the Xishuangbanna sites. Detailed age information for the sites is provided in *SI Appendix*, Table S3.

Wet Nitrogen Deposition Data. We collected published annual wet nitrogen deposition data in China based on rain collection measurements performed from 2000 to 2010. In all, 167 nitrogen deposition measurement sites in China were included. Moreover, we collected wet nitrogen deposition data from the Acid Deposition Monitoring Network in East Asia. The mean monthly value for wet nitrogen deposition was measured continuously from 2000 to 2009 by the Acid Deposition Monitoring Network in East Asia. In 2009, wet nitrogen deposition monitoring was conducted at 54 sites (remote, 20; rural, 13; urban, 21) following a set of uniform monitoring guidelines and technical manuals (www.eanet.asia/product/index.html).

In total, 221 wet nitrogen deposition observation sites were collected in the Asian region (*SI Appendix*, Fig. S8). Seven of these sites are forest flux sites for which in situ continuous wet nitrogen deposition measurements are available. We then used the observed values from sites located within a 1° circular buffer area around the forest flux site to supply data for the sites for which measurements of wet nitrogen deposition were missing. The results showed a good relationship between the observed and averaged wet nitrogen deposition from the sites in the 1° buffer circle if the wet nitrogen deposition was less than 40 kg N ha^{-1} yr^{-1}, although an underestimate of ~40% was detected (*SI Appendix*, Fig. S9). A total of 20 sites with wet nitrogen deposition data were obtained after integration, as shown in *SI Appendix*, Table S3. We conducted a type II regression to analyze the correlation between NEP and wet nitrogen deposition. Similarly, we averaged the data from the 221 wet nitrogen deposition observation sites into 10° latitude bins for our integrated analysis.

East Asian Monsoon Forest NEP Estimation. The total East Asian monsoon forest NEP was the product of the average forest NEP and the forest areas of East Asian monsoon region. The forest areas were estimated based on MODIS land-cover products (MODIS Land Cover Type Yearly L3 Global 0.05Deg CMG V051, MCD12C1-2008) downloaded from the National Aeronautics and Space Administration Land Processes Distributed Active Archive Center (https://lpdaac.usgs.gov/get_data). The MODIS land-cover products, in Hierarchical Data Format-Earth Observing System files, were projected onto a tile-based sinusoidal grid using the MODIS Reprojection Tool. The East Asian monsoon region at latitudes from 20° to 40°N and at longitudes from 100° to 145°E was then abstracted from this grid, and the abstracted land cover was reclassified into forest and nonforest. The definition of forests in this study was specified by the following categories in the MODIS land cover: evergreen broad-leaved forests, evergreen coniferous forests, deciduous broad-leaved forests, deciduous coniferous forests, and mixed forests.

Global and Asian Forest NEP Estimation. Global and Asian total forest NEP was derived from Jung's global NEP data product (33), which was based on the space/time interpolation of flux tower observations using a model tree ensemble regression trained with satellite FAPAR and gridded climate field predictors. Here, we multiplied the NEP of each pixel with the forest area by the MODIS reclassified forest land cover, as defined above, to estimate global and Asian total forest NEP.

Process-Oriented Models. NEP values estimated from three different models [LPJ (12), ORCHIDEE (13) and CLM4CN (14)] were used in this study. These models only consider changes in climate and increasing atmospheric CO_2 (37). We used the MODIS reclassified forest land cover as defined above to extract the forest NEP for the East Asian monsoon region, the Asian region, and globally from the three model estimates.

Data Analysis. All data were analyzed with SPSS 16.0 statistical software. We used a one-way ANOVA and least-significant difference test (43) ($P < 0.05$) to analyze the NEP differences between seven latitudinal bins in the Asian region and to analyze the NEP differences between the Asian, European, and North American regions. We used an independent-samples t test ($P < 0.05$)

to analyze the NEP differences between the Asian and North American regions. We used a polynomial regression to analyze the relationship of NEP to age and a type II regression (smatr package in R software) to analyze the relationship of NEP to wet nitrogen deposition. All figures were drawn using Sigma Plot 10.0 software. The spatial distribution figures for the sites were plotted with ArcGIS 10.0 software.

ACKNOWLEDGMENTS. We thank M. Jung for providing a global net ecosystem exchange assessment distribution map based on Model Tree Ensemble information; S. Levis and B. Poulter for providing carbon cycle modeling simulation results; the Network Center for Acid Deposition Monitoring Network in East Asia (EANET) for providing EANET Data on the Acid Deposition in the East Asian Region; S. G. Li for comments and discussions; X. H. Wang for checking model data; H. J. Nan and Z. Z. Zeng for checking the European and American carbon flux data; and the editor and three anonymous reviewers' valuable comments and constructive suggestions on the previous version of the manuscript. This study was supported by the National Key Research and Development Program (Grant 2010CB833504), the Chinese Academy of Sciences Strategic Priority Research Program (Grant XDA05050602), and the Key Program of National Natural Science Foundation of China (Grant 31290221).

1. Houghton JT, et al., eds (2001) *Climate Change 2001: The Scientific Basis.* (Cambridge Univ Press, Cambridge, UK).
2. Tans PP, Fung IY, Takahashi T (1990) Observational contrains on the global atmospheric CO_2 budget. *Science* 247(4949):1431–1438.
3. Ciais P, Tans PP, Trolier M, White JWC, Francey RJ (1995) A large northern hemisphere terrestrial CO_2 sink indicated by the $^{13}C/^{12}C$ ratio of atmospheric CO_2. *Science* 269(5227):1098–1102.
4. Pan YD, et al. (2011) A large and persistent carbon sink in the world's forests. *Science* 333(6045):988–993.
5. Phillips OL, et al. (1998) Changes in the carbon balance of tropical forests: Evidence from long-term plots. *Science* 282(5388):439–442.
6. Lewis SL, et al. (2009) Increasing carbon storage in intact African tropical forests. *Nature* 457(7232):1003–1006.
7. Wu GX (2007) The influence of mechanical and thermal forcing by the Tibetan Plateau on Asian climate. *J Hydrometeorol* 8(4):770–789.
8. Duan AM, Wu GX (2005) Role of the Tibetan Plateau thermal forcing in the summer climate patterns over subtropical Asia. *Clim Dyn* 24(7–8):793–807.
9. Huang RH, Zhou LT, Chen W (2003) The progresses of recent studies on the variabilities of the East Asian Monsoon and their causes. *Adv Atmos Sci* 20(1):55–69.
10. Food and Agriculture Organization (2001) *Global Ecological Zoning for the Global Forest Resources Assessment 2000* (Food and Agriculture Organization, Rome), pp 128–132.
11. Galloway JN, et al. (2004) Nitrogen cycles: Past, present, and future. *Biogeochemistry* 70(2):153–226.
12. Sitch S, et al. (2003) Evaluation of ecosystem dynamics, plant geography and terrestrial carbon cycling in the LPJ dynamic global vegetation model. *Glob Change Biol* 9(2):161–185.
13. Krinner G, et al. (2005) A dynamic global vegetation model for studies of the coupled atmosphere-biosphere system. *Global Biogeochem Cycles* 19(1):GB1015.
14. Lawrence DM, et al. (2011) Parameterization improvements and functional and structural advances in version 4 of the community land model. *J Adv Model Earth Syst* 3(1):M03001.
15. Thornton PE, et al. (2002) Modeling and measuring the effects of disturbance history and climate on carbon and water budgets in evergreen needleleaf forests. *Agric Meteorol* 113(1–4):185–222.
16. Dore S, et al. (2010) Carbon and water fluxes from ponderosa pine forests disturbed by wildfire and thinning. *Ecol Appl* 20(3):663–683.
17. Pan YD, et al. (2011) Age structure and disturbance legacy of North American forests. *Biogeosciences* 8(3):715–732.
18. Wolf S, Eugster W, Potvin C, Turner BL, Buchmann N (2011) Carbon sequestration potential of tropical pasture compared with afforestation in Panama. *Glob Change Biol* 17(9):2763–2780.
19. Peichl M, Brodeur JJ, Khomik M, Arain MA (2010) Biometric and eddy-covariance based estimates of carbon fluxes in an age-sequence of temperate pine forests. *Agric Meteorol* 150(7–8):952–965.
20. Goulden ML, et al. (2011) Patterns of NPP, GPP, respiration, and NEP during boreal forest succession. *Glob Change Biol* 17(2):855–871.
21. Chen JM, et al. (2003) Spatial distribution of carbon sources and sinks in Canada's forests. *Tellus Ser B* 55(2):622–641.
22. State Forestry Bureau (2010) *Forest Resources Statistics of China for Periods 2004–2008.* (China's Forestry Publishing House, Beijing), Chinese.
23. Food and Agriculture Organization (2010) *Global Forest Resources Assessment 2010* (Food and Agriculture Organization, Rome), pp 9–44.
24. Stoy PC, et al. (2008) Role of vegetation in determining carbon sequestration along ecological succession in the southeastern United States. *Glob Change Biol* 14(6): 1409–1427.
25. Zhu ZL (1990) *China Soil Nitrogen* (Jiangsu Sci Technol Press, Nanjing), pp 3–5. Chinese.
26. Thomas RQ, Canham CD, Weathers KC, Goodale CL (2010) Increased tree carbon storage in response to nitrogen deposition in the US. *Nat Geosci* 3(1):13–17.
27. LeBauer DS, Treseder KK (2008) Nitrogen limitation of net primary productivity in terrestrial ecosystems is globally distributed. *Ecology* 89(2):371–379.
28. Bowden RD, Davidson E, Savage K, Arabia C, Steudler P (2004) Chronic nitrogen additions reduce total soil respiration and microbial respiration in temperate forest soils at the Harvard forest. *For Ecol Manage* 196(1):43–56.
29. Olsson P, Linder S, Giesler R, Högberg P (2005) Fertilization of boreal forest reduces both autotrophic and heterotrophic soil respiration. *Glob Change Biol* 11(10): 1745–1753.
30. Mo JM, et al. (2008) Nitrogen addition reduces soil respiration in a mature tropical forest in southern China. *Glob Change Biol* 14(2):403–412.
31. Dentener F, et al. (2006) Nitrogen and sulfur deposition on regional and global scales: A multimodel evaluation. *Global Biogeochem Cycles* 20(4):GB4003.
32. Reay DS, Dentener F, Amith P, Grace J, Feely RA (2008) Global nitrogen deposition and carbon sinks. *Nat Geosci* 1(7):430–437.
33. Jung M, et al. (2011) Global pattern of land-atmosphere fluxes of carbon dioxide, latent heat, and sensible heat derived from eddy covariance, satellite, and meteorological observations. *J Geophys Res* 116(G3):G00J07.
34. Chapin FS, III, Matson PA, Mooney HA, eds (2002) *Principles of Terrestrial Ecosystem Ecology.* (Springer, New York), pp 142–144.
35. Piao SL, et al. (2013) Evaluation of terrestrial carbon cycle models for their response to climate variability and to CO_2 trends. *Glob Change Biol* 19(7):2117–2132.
36. Denman K, et al. eds (2007) *Climate Change 2007: The Physical Science Basis.* (Cambridge Univ Press, Cambridge, UK).
37. Piao SL, et al. (2009) Spatialtemporal patterns of terrestrial carbon cycle during the 20th century. *Global Biogeochem Cycles* 23(4):GB4026.
38. Webb EK, Pearman GI, Leuning R (1980) Correction of flux measurements for density effects due to heat and water vapour transfer. *Q J R Meteorol Soc* 106(447):85–100.
39. Reichstein M, et al. (2005) On the separation of net ecosystem exchange into assimilation and ecosystem respiration: Review and improved algorithm. *Glob Change Biol* 11(9):1424–1439.
40. Falge E, et al. (2001) Gap filling strategies for defensible annual sums of net ecosystem exchange. *Agric Meteorol* 107(1):43–69.
41. Matsuura Y, et al. (2007) in *Proceedings of the Seventh International Conference on Global Change: Connection to the Arctic (GCCA-7)* (International Arctic Research Center, Fairbanks, AK), pp 258–261.
42. Arneth A, et al. (2002) Compararive ecosystem-atmosphere exchange of energy and mass in a Ruropean Russian and a central Siberian bog П. Interseasonal and interannual variability of CO_2 fluxes. *Tellus Ser B* 54(5):514–530.
43. Fisher RA (1936) The use of multiple measurements in taxonomic problems. *Ann Eugen* 7(2):179–188.